Holocene transgression recorded by sand composition in the mesotidal Galician coastline (NW Spain)

José Arribas,[1] Ángela Alonso,[2] Jose Luis Pagés[2] and Laura González-Acebrón[1]

Abstract

This study confirms several inferences regarding Holocene coastal dynamics and climate through a petrographic modal analysis of 60 Holocene sand samples recovered in seven sites along the NW coast of the Iberian Peninsula. Fluvial sand can be discriminated from more mature intertidal and aeolian sand according to texture and composition. Fluvial sand contains soil products and coastal sand has significant bioclasts. Quartzofeldspathic sand appears in the western area (produced by the erosion of granite and granitoid), and quartzolithic sand occurs in the eastern area (produced by the erosion of metasediment). Changes in sand composition during Holocene deposition are manifested by an increase in modern carbonate clasts (MC) correlated with the Holocene transgression. Episodes of faster sea-level rise and subsequent erosion of surrounding cliffs are indicated by the preservation of high proportions of feldspar in intertidal sand. In contrast, fluvial sand is characterized by greater quartz enrichment. These inferences were confirmed by petrographic indices (carbonate clasts/total clasts, MC/T; total feldspars/monocrystalline quartz, F/Qm; and plagioclase/total feldspars, P/F). The different maturity of intertidal and aeolian sands is revealed by their variable quartz contents, despite similar proportions of plagioclase and K-feldspar. This suggests mechanical abrasion as the main factor controlling maturity. In contrast, fluvial sand shows depleted plagioclase contents as the result of inland weathering processes. Intertidal, beach and aeolian sands are essentially the products of the erosion of coastal cliffs and head deposits, with only the scarce contribution of fluvial drainages. The long-distance transport of Galician coastal sands is discarded based on the close relationship between their composition and that of local sand sources. Our findings indicate that short-distance transport of sediments from the west closed off coastal wetlands and occluded estuarine mouths during the Holocene transgression by deposition on sediment-trap zones along the irregularly shaped Galician coast.

Keywords

coastal sands, coastal dynamics, Galicia, Holocene transgression, provenance, sand composition, Spain

Introduction

The genesis of recent and modern (i.e. Holocene) deposits has recently generated worldwide interest, since understanding related processes will allow us to more reliably predict future changes. During the last few decades, special efforts have been made to identify climate fluctuations and their consequences in fields related to vegetation (Birks, 2003; Froyd, 2005), micropaleontology (e.g. Anderson, 1995; Smol and Cumming, 2000), isotopes (e.g. Hong *et al.*, 1995) and sedimentology (e.g. Culver *et al.*, 2007). In these fields, sensitive signatures are used as climate indicators.

The northern coast of Galicia and western area of Asturias, in the northwest sector of the Iberian Peninsula (Figure 1), is an abrupt mesotidal wave-dominated coast, where sedimentation shows a discontinuous distribution in estuaries, barriers, coastal lagoons, beaches and pocket beaches. The Holocene record has been mainly interpreted as infilling sequences of estuaries or back-barrier coastal wetlands (Alonso and Pagés, 2000; García Antón *et al.*, 2006; Bao *et al.*, 2007).

The composition of clastic deposits is the final outcome of the cumulative effects of highly interrelated factors (Johnsson, 1993) that mainly involve source lithology, chemical weathering, hydraulic sorting and abrasion. Thus, detrital modes can be used to decipher these factors. Studies on modern sand composition enable direct comparison between the source system and the sandy products (Ibbeken and Schleyer, 1991; Arribas and Tortosa, 2003) and also serve to monitor other factors. Climate and vegetation control the intensity of chemical weathering of the source rock (e.g. Nestbitt *et al.*, 1997). Physiography substantially affects denudation rates, and therefore, the weathering interval (e.g. Grantham and Velbel, 1988; Johnsson *et al.*, 1991). Some minerals and clastic particles such as feldspars or rock fragments are sensitive to climate conditions (e.g. Krynine, 1950; Todd, 1968; Suttner and Dutta, 1986), and thus, the bulk composition of sands could be used as a climate proxy.

To address the role of factors such as source area lithology, sedimentary environment and climate on sand composition, this paper describes sand composition and textures of Holocene deposits recorded at seven sites of the northwestern coast of the Iberian Peninsula (Traba, Baldaio, Pto. Coruña, Miño, Pantín, Viveiro and

[1]Universidad Complutense de Madrid – IGE, C.S.I.C., Spain
[2]Universidad de A Coruña, Spain

Corresponding author:
José Arribas, Departamento de Petrología y Geoquímica, Universidad Complutense de Madrid – IGE, C.S.I.C., 28040-Madrid, Spain
Email: arribas@geo.ucm.es

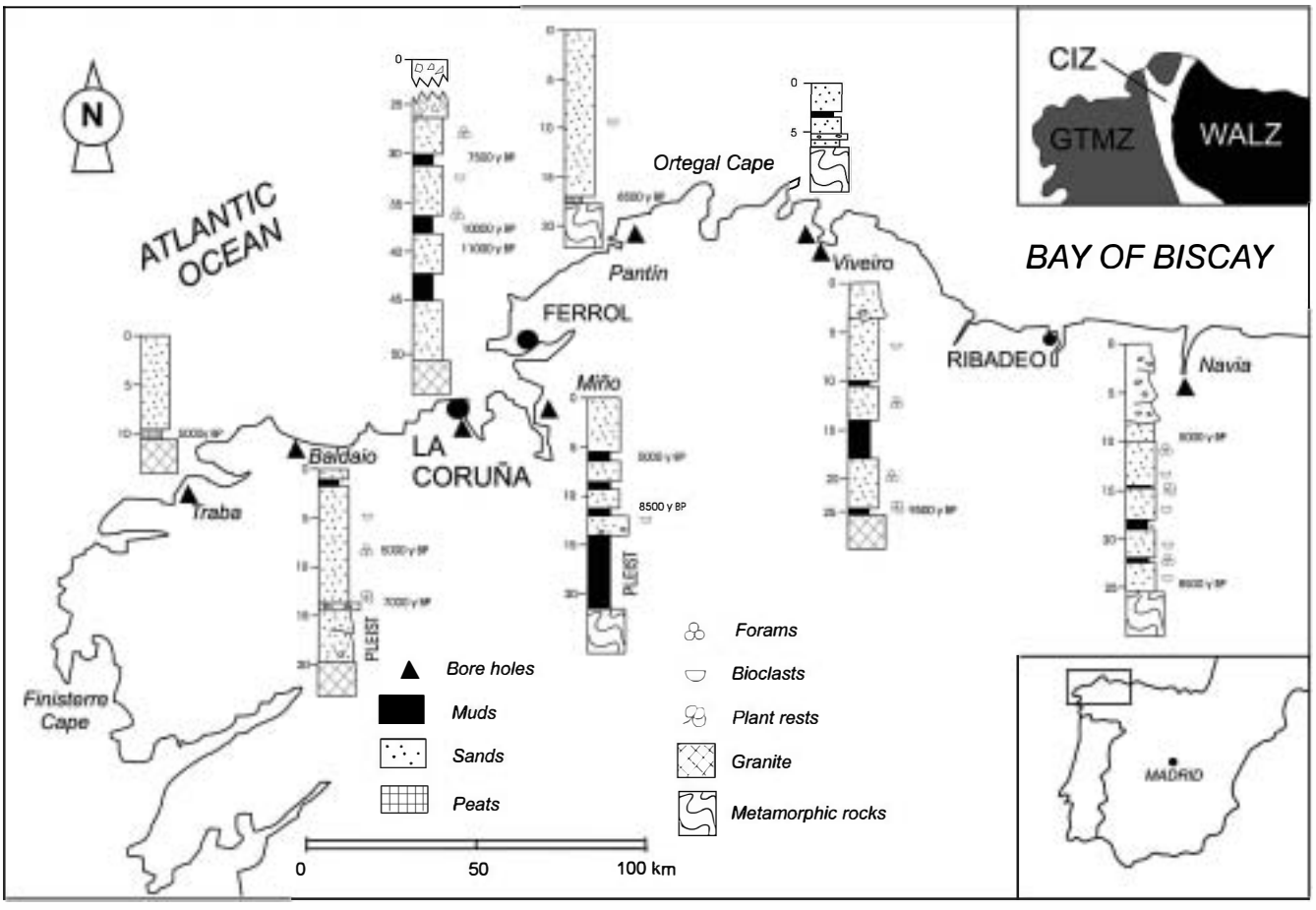

Figure 1. Location map of the study area and the sites of the Holocene record analysed. GTMZ, Galicia Tras os Montes Zone domain; CIZ, Central Iberian Zone domain; WALZ, Western Asturian Leonese Zone domain

Navia, Figure 1). Further insight into Holocene processes was obtained by comparing our results with those of other studies of the same stratigraphic records (e.g. Alonso and Pagés, 2000; Alonso *et al.*, 2003; Delgado *et al.*, 2003; Pagés *et al.*, 2003; García Antón *et al.*, 2006; Bao *et al.*, 2007).

General setting

Climate, waves, tides and sea level

The climate of the coastal area of Galicia and Asturias is oceanic with abundant regular rainfall (mean 1000 to 2000 mm/yr), and mild temperatures that vary within a narrow range (from averages of 8–9°C in January to 18–;19°C in July). Wet warm winds from the west are dominant (Castillo Rodríguez *et al.*, 2006). According to these climate conditions, mechanical and chemical weathering can be considered as moderate (Wilson, 1969).

From winter to summer, wave energy varies greatly. The average annual significant height (Hs) is 2.7 m, and the peak period (Tp) is 11.1 s. Wave provenance remains rather constant throughout the year, with 75% arising in the W–NNW sector (data from the directional Sea Watch Buoy of Estaca de Bares, located at 44°3.9′N, 7°37.1′W, with a sea floor depth of 382 m; http://www.puertos.es/es/oceanografia_y_meteorologia/banco_de_datos/oleaje.html).

The Galician coast is a mesotidal wave-dominated coast with maximum tides of 4.40 m recorded in springtime (data from Gijón seaport, year 2002). Average rates of sea-level change can be obtained from the records of tide gauges installed along the northern coast of Spain (available through the web page of the Permanent Service of Mean Sea Level, http://www.pol.ac.uk/psmsl/datainfo). In the Atlantic, these sea-level rises have been estimated at 1.5 mm/yr in A Coruña during the last 62 available years (1944–2005), to 2.6 mm/yr in Vigo during the period 1944–2001 (58 years). In the Bay of Biscay (Cantabrian), Santander seaport records a sea-level rise of 2.2 mm/yr for the period 1944–2001 (57 years). These data are slightly higher than averages for northern Europe (1 to 2.5 mm/yr; Zerbini, 2000).

Physiography and lithology

The northwest coast of Spain (Galicia) shows a rugged morphology, with high promontories, cliffs up to 100 m high, headlands, embayed beaches and funnel-shaped incisions (*rías*). The coast is developed on igneous and metamorphic rocks of the Variscan Chain (Macizo Ibérico) and shows several domains derived from a highly complex collision orogen (e.g. Arenas *et al.*, 1986). Three main domains are represented: (1) the Galicia Tras os Montes Zone (GTMZ), (2) the Central Iberian Zone (CIZ), and (3) the Western Asturleonese Zone (WALZ) (Figure 1).

Table 1. Sizes of the drainage basins and surface area percentages of their representative lithologies

	Total (km^2)	1	2	3	4	5
Traba	18.82	100.0	0.0	0.0	0.0	0.0
Baldaio	41.13	74.0	10.9	8.1	7.1	0.0
Pto.	266.15	19.7	0.0	80.3	0.0	0.0
Miño	47.90	54.3	7.1	35.5	3.1	0.0
Pantín	8.55	12.4	50.2	37.5	0.0	0.0
Vivero	298.50	47.1	0.0	45.8	7.2	0.0
Navia	1906.56	0.6	0.0	48.4	49.4	1.6

1, Granites, granodiorites and gneisses; 2, gabres and amphybolites; 3, slates, schists and shales; 4, sandstones and metagrauvakes; 5, carbonates (limestones and dolostones)

The eastern zone of the area of study corresponds to the western limit of the Gulf of Biscay. This coastal segment is an E–W straight coast composed of low-grade Cambro-Ordovician metamorphicrocks (schists, quartzites, shales and sandstones) from the WALZ domain. One of the most significant fluvial courses is the Navia River, which is 105 km long. The drainage basins of these rivers are developed on the Cambro-Ordovician WALZ domain.

The Galician coast is an abruptly shaped coastline with dominant NW–SE and NE–SW orientations and high cliffs. Its substrate is composed of Cambro-Ordovician and Silurian metasediments and granites from the WALZ domain, gneisses and quartzites from the CIZ zone, and granites, gneisses, mafic and ultramafic rocks from the GTMZ domain, in the westernmost area of study. Rivers are no more than 50 km long, and frequently form *rías* at their mouths. Inland drainage areas are mainly made up of granites and locally of metasediments and mafic metamorphic rocks.

Drainage basins from the inland fluvial courses of the different sampling sites are highly variable in surface area and percentage drained lithologies (Table 1). Those of Navia, Vivero, Miño and Pto. Coruña are wider drainage basins. Each has a main collector showing constant flow. On the contrary, the smaller catchments (Traba, Baldaio and Pantín) are drained by short streams showing sporadic flow. Coarse-grained rocks (1 and 2 in Table 1), especially granites, are the most abundant potential sources of detritus to coastal sand at the respective sampling sites.

Sedimentary record

The morphology of the coastline is predominantly inherited from former high stands. During the last glacial period, the incision of fluvial systems was developed, leading during the Holocene flooding to the formation of rías, and displaying a wide outer marine zone and an inner estuary. The coastal plain was flooded during the postglacial period, and estuaries were already inundated at the beginning of the Holocene. The sea-level rise was fast during the early Holocene (up to 5 mm/yr from 8500 to 7500 cal. yr BP), decelerating thereafter (3.5 to 2 mm/yr in the period 7500 to 5000 yr cal. BP) until its almost stabilization (Alonso *et al.*, 2003; Pagés *et al.*, 2003, 2005). This deceleration induced the replenishment of estuaries and the formation of several beach-barrier complexes in the most open areas of the coast and on the outer parts of the rías. This process caused the concurrent erosion of former sedimentary units in open coasts and cliffs (Lorenzo *et al.*, 2007). Sea-level rise continued thereafter (up to 1.5 mm/yr).

As a consequence, Quaternary outcrops are scarce and appear only as disconnected remains (palaeobeaches and head deposits of Late Pleistocene age, aeolian sands, peats and flash-flood deposits of the Holocene). Owing to the scarcity of Holocene outcrops, this work is based on cores obtained in estuaries (Navia, Vivero), barrier-lagoon complexes (Miño, Pantín, Baldaio, Traba) and the outer marine zone of the ría of Ares (Pto. Coruña). Boreholes drilled the entire sedimentary cover, as far as the granites and metamorphic rocks comprising the basement (Figure 1). Radiocarbon dating demonstrated that the Late Pleistocene is represented in the bases of three of the cores. These cores, designated according to their corresponding locations, were Baldaio, in which fluviatile conglomerates and sands in upwards fining sequences appeared; Miño, showing muddy facies and intercalated immature conglomerates representing flash-flood channels in flood flats; and Pto. Coruña, containing fluviatile immature conglomerates and muds, which in the upper portion were dated as Younger Dryas.

In some of the boreholes, the entire Holocene sequence is represented. The Holocene record in Navia and Vivero indicates the replenishment of inner estuaries that were flooded at the beginning of the Holocene. Facies correspond to intertidal mixed flats passing upward in Navia to a fluvial-dominated estuary. Baldaio and Miño correspond to tidal flats in a back-barrier, very shallow-lagoon environment, while Pantín and Traba can be considered as coastal lakes or back-dune wetlands with no or only a minor connection to the sea throughout their history. At Pto. Coruña, only the early Holocene is represented; sedimentation took place in tidal flats and intertidal channels developed on the wide platform formed during low sea-level stages and were inundated during the first stages of postglacial flooding.

Petrographic procedures and grain types

Sixty sand samples were collected from eight mechanical cores drilled on the coastal wetlands of Traba (10.6 m) and Pantín (16.5 m); the shallow lagoon complexes of Baldaio (19.6 m) and Miño (21.9 m), the estuaries of Vivero (26.1 m) and Navia (25.2 m), and in the outer part of the Ria de Ares (Pto. Coruña, 51.5 m) (Figure 1). These cores were radiocarbon-dated at several depths, providing ages from 43 000 BP (Miño) and 5000 BP (Traba) to the present.

Sands were washed with fresh water to eliminate salts, and wet sieved across the range 2–0.062 mm to remove mud particles (<0.062 mm) and scarce granules (>2 mm). Samples with

high quantities of organic matter were etched with diluted H_2O_2. The sand fraction was air-dried, artificially cemented with epoxy resin, and thin-sectioned. Each thin section was etched with HF and stained by immersion in Na-cobaltinitrite solution to identify feldspars (Chayes, 1952). Alizarine red-S and ferricyanide solution (Lindholm and Finkelman, 1972) were used for carbonate identification. Textures of the sediments (grain size, sorting and quartz grain roundness) were estimated on thin sections using comparative schemes. A petrographic data base was established by counting more than 300 grains in each thin section according to the Gazzi-Dickinson (G-D) method (Ingersoll *et al.*, 1984). Data were tabulated following Zuffa (1985), which allows the ambivalent treatment of data as both the traditional and G-D method. Twenty-eight grain classes were considered and grouped into three main categories: (1) AN, ancient non-carbonates; (2) MC, modern carbonates; and (3) MN, modern non-carbonates.

Ancient non-carbonates (AN) are the most abundant grain type in the sands; this category includes quartz grains (mono- and polycrystalline types), monocrystalline K-feldspars and albites. Twinned grains of plagioclases are commonly both as fresh and variably altered to clay minerals. Micas (muscovite, biotite and chlorite) are very abundant locally. All AN grains occur as monominerals and as the crystal constituents of phaneritic rock fragments (i.e. granites, gneisses) (Table 2). Aphanitic rock fragments (L grains in Table 2) in some samples are abundant (e.g. in Navia) and consist of shale, phyllite and chert. In addition, dense minerals may occur as associations comprising tourmaline, zircon, apatite, garnet, hornblende, brookite, rutile, anatase and opaque minerals that characterize felsic plutonic sources (Pettijohn *et al.*, 1972). In some samples, these minerals are very abundant and account for 5% of the total.

Modern carbonates (MC) are represented by bioclasts, mainly of molluscs (abraded lamellibranchian shells and a few unspecified gastropods); echinoderms, foraminifera, red algae, bryozoans and ostracods also appear but in lower proportions. Commonly, shells are micritized, which makes their identification difficult. Locally, this category is highly represented in the sands and amounts to 58% of total grains. In some samples, these grains are absent.

Modern non-carbonates (MN) consist mainly of silty-clayey grains with irregular edges and large grain sizes. Concretions of Fe-oxides (alterites) are locally abundant (5%), representing clear land side supplies. These grains occur in sands related to the infill of channels from intertidal mixed flats. Glauconite was identified as trace grains (<1%) in sands from the Miño record.

Several compositional parameters and indices have been considered to describe the modal composition of sands using binary (carbonate to total grains – C/T – versus ancient non-carbonates to total grains – AN/T –, modified from Di Giulio and Valloni, 1992) and ternary diagrams (QFR, Pettijohn *et al.*, 1972; QmFLt and QmKP, Dickinson *et al.*, 1983; and Qmr Qmo Qp, according to the criteria of Basu *et al.*, 1975). In addition, indices such as Rg/Rt (coarse crystalline rock fragments/total rock fragments), F/Qm (feldspars/monocrystalline quartz), and P/F (plagioclase/feldspars) were calculated to clarify variations in sand composition through time.

Point-count raw data and recalculated variables are shown in Table 2.

Textures of sands

Grain sizes in the sand deposits vary according to the environment (Table 3). Aeolian and intertidal deposits show homogeneous grain-size intervals, mainly from 177 to 350 μm. These consist of unimodal deposits, which are well or very well sorted with large populations of high quartz roundness. Bimodal sands are also present and were interpreted as the result of mixing of aeolian and intertidal sands. Grain size decreases where intertidal environments are related to mixed flats, or may increase in association with fluvial channel infill. In both cases, sorting decreases and the angular quartz grain population stabilizes (Table 3).

Fluvial deposits show wider grain size intervals; from very fine (fluvial flats or swamps areas) to very coarse sands (lag deposits in channels). These deposits are very poorly sorted and quartz roundness is low. The lack of roundness in quartz grains is, therefore, indicative of sand directly arising from the drainage basin.

Locally, embayed quartz grains were identified in fluvial channel sands in association with alterite grains, suggesting an origin related to weathering profiles formed in drainage areas (Cleary and Conolly, 1971; Johnsson, 1990).

Composition of sands

The composition of the total grain population (Figure 2) is siliciclastic (AN) with variable amounts of bioclastic carbonate grains (MC) that usually do not exceed 25% of total clasts. The ancient siliciclastic character of the sand reflects an origin related to main land supplies from the erosion of drainage areas and sea cliffs, with the scarce contribution of modern carbonate bioclasts. Hybrid sand containing more than 25% bioclasts is also observed in the Pantín, Baldaio and Navia records. Mixing between these two end-member contributors of sand is reflected in Figure 2 in the continuous plots of sands along the diagonal line of the diagram. Sand from Pto. Coruña differs from this general distribution pattern in that it shows the presence of substantial amounts of modern silty-clayey drapes (MN).

The absence of bioclasts in sand can be correlated with fluvial deposits, as occurs at the base of the successions of Pto. Coruña, Miño, Baldaio and Vivero-Puente. At the top of this last section, bioclasts are also absent. In aeolian deposits (mainly in Traba, and Pantín), the content of bioclasts is low and almost constant through the sections. Intertidal deposits (e.g. Navia, top of Pto. Coruña, and top of Baldaio sections) show more scattered bioclast contents, although these increase towards the top of the sequences (Pto. Coruña and Baldaio).

Main modal sand composition (QFR; QmFLt)

The ancient siliciclastic components (AN) of all the analysed sands of the Galician coast are quartzofeldspathic. This character is manifested in the sand plots close to the QF line in the QFR diagram; and even closer to the line in the QmFLt diagram (Figure 3). Differences between these two diagrams reflect the presence of coarse-grained rock fragments in the sands. Quartzofeldspathic petrofacies reflect an origin related to erosion of coarse crystalline rocks (granitoid) that constitute the main lithology of the coastal cliffs and drainage basins (CIZ of the Iberian Massif).

Table 2. Results of the petrographic modal analysis

		Traba					
		TRA-9,60	TRA-8,8	TRA-6,60	TRA-5,2	TRA-3,20	TRA-0,80
AN							
Q							
Qmr	Monocrystalline non-undulose quartz	147	130	128	143	128	131
Qmo	Monocrystalline undulose quartz	39	54	52	40	50	61
Qp2-3	Polycrystalline quartz (2-3 crystals)	21	15	8	17	12	7
Qp>3	Polycrystalline quartz (>3 crystals)	4	9	13	9	11	11
Qrm	Quartz in low and medium meta. grade rock fragm.						
Qrp	Quartz in plutonic rock fragment	1	3	3	5	1	4
Qrg	Quartz in gneissic rock fragment						
Qrs	Quartz in sandstone						
K							
Ks	K-feldspar (single crystal)	31	39	43	31	37	34
Krm	K-feldspar in low and medium meta. grade rock fragm.						
Krp	K-feldspar in plutonic rock fragment	2	2	5	4	1	1
Krg	K-feldspar in gneissic rock fragment						
P							
Ps	Plagioclase (single crystal)	19	27	18	21	27	28
Prm	Plagioclase in low and medium meta. grade rock fragm.						
Prp	Plagioclase in plutonic rock fragment			1	1	1	1
M							
Bi	Biotite (single crystal)						
Mu	Muscovite (single crystal)	2					
Cl	Chlorite (single crystal)						
Mrm	Mica in low and medium meta. grade rock fragm.						
L							
Ch	Unspecified chert						
Sh	Shale and fillites						
Dm	Dense minerals (unspecified)						
MC							
	Molusc	13	16	23	26	18	14
	Echinoderm	4	1	3	3	10	6
	Foram.; red algae; briozoo.; ostracods						
	Indeterminate bioclast	22	9	12	10	7	8
MN							
	Silty-clay soft grains, glauconite Fe-Oxides, alterite						
	Total	305	305	309	310	303	306
	MC/T	0.13	0.09	0.12	0.13	0.12	0.09
	AN/T	0.87	0.91	0.88	0.87	0.88	0.91
	Q	79.9	74.6	74.2	77.1	75.0	75.5
	F	18.9	23.7	22.5	19.2	23.9	22.3
	R	1.1	1.8	3.3	3.7	1.1	2.2
	Qm	80.3	75.6	75.3	79.0	75.4	77.0
	F	19.7	24.4	24.7	21.0	24.6	23.0
	Lt	0.0	0.0	0.0	0.0	0.0	0.0
	Qm	80.3	75.6	75.3	79.0	75.4	77.0
	K	12.5	14.7	17.7	12.9	14.2	12.6
	P	7.2	9.7	7.0	8.1	10.4	10.4
	Qmr	69.7	62.5	63.7	68.4	63.7	62.4
	Qmo	18.5	26.0	25.9	19.1	24.9	29.0
	Qp	11.8	11.5	10.4	12.4	11.4	8.6
	Rg/Rt	1.00	1.00	1.00	1.00	1.00	1.00
	F/Qm	0.25	0.32	0.33	0.27	0.33	0.30
	P/F	0.37	0.40	0.28	0.39	0.42	0.45

(Continued)

Table 2. (Continued)

		Baldaio											
		BAL-19,6	BAL-18,25	BAL-17,2	BAL-15,1	BAL-14,2	BAL-13,0	BAL-11,4	BAL-9,6	BAL-7,5	BAL-5,4	BAL-3,7	BAL-2,0
AN													
Q													
Qmr	Monocrystalline non-undulose quartz	97	135	151	161	97	87	96	111	76	60	79	114
Qmo	Monocrystalline undulose quartz	46	42	51	47	28	28	28	34	28	30	26	37
Qp2-3	Polycrystalline quartz (2-3 crystals)	34	18	21	10	20	11	14	17	19	10	10	12
Qp>3	Polycrystalline quartz (>3 crystals)	26	15	12	12	24	16	12	17	19	20	14	16
Qrm	Quartz in low and medium meta. grade rock fragm.	3	1			4				1		1	
Qrp	Quartz in plutonic rock fragment	6	5	6	4	13	2	3	4	3	1	1	2
Qrg	Quartz in gneissic rock fragment												2
Qrs	Quartz in sandstone												
K													
Ks	K-feldspar (single crystal)	50	49	39	46	47	35	40	38	29	31	38	29
Krm	K-feldspar in low and medium meta. grade rock fragm.												
Krp	K-feldspar in plutonic rock fragment	4	5	4	3	5	4		2	1		2	5
Krg	K-feldspar in gneissic rock fragment												1
P													
Ps	Plagioclase (single crystal)	34	30	24	21	23	24	21	18	19	15	18	25
Prm	Plagioclase in low and medium meta. grade rock fragm.												
Prp	Plagioclase in plutonic rock fragment	2		1		2	1		1	1	2	1	2
M													
Bi	Biotite (single crystal)	4	1	1	1	40	3	9	3	2	2	1	1
Mu	Muscovite (single crystal)	9	10	1	2	14	3	3	3	6	3	8	2
Cl	Chlorite (single crystal)												
Mrm	Mica in low and medium meta. grade rock fragm.	2	1			5					1	2	
L													
Ch	Unspecified chert		1				1		1	2			
Sh	Shale and fillites	3	3			4	1	1	2	2	1	1	
Dm	Dense minerals (unspecified)	14	7	6	7	4	1	2	3	2	2	4	5
MC													
	Molusc					12	64	50	44	82	84	123	40
	Echinoderm					4	22	14	7	12	18	16	3
	Foram.;red algae; briozoo.; ostracods					1			2		2		2
	Indeterminate bioclast					5	10	16	11	14	30	75	23
MN													
	Silty-clay soft grains, glauconite Fe-Oxides, alterite	11		3					1	2		1	
	Total	345	323	320	314	352	313	309	319	320	312	421	321
	MC/T	0.00	0.00	0.00	0.00	0.06	0.31	0.26	0.20	0.34	0.43	0.51	0.21
	AN/T	0.97	1.00	0.99	1.00	0.94	0.69	0.74	0.80	0.66	0.57	0.49	0.79
	Q	66.1	69.2	76.1	75.7	62.1	68.1	69.8	73.5	72.0	70.2	66.8	73.1
	F	27.4	25.9	20.4	22.0	25.7	28.1	28.4	22.9	24.0	26.9	29.0	22.0
	R	6.5	5.2	3.6	2.3	12.1	4.3	1.9	4.1	5.0	2.9	4.1	4.9
	Qm	69.5	71.1	78.0	77.0	69.7	68.6	71.2	74.7	73.0	71.2	68.6	74.7
	F	29.5	27.6	22.0	23.0	28.8	30.5	28.4	24.1	25.0	28.2	30.9	25.3
	Lt	1.0	1.3	0.0	0.0	1.5	1.0	0.5	1.2	2.0	0.6	0.5	0.0
	Qm	70.2	72.0	78.0	77.0	70.7	69.2	71.5	75.6	74.5	71.6	68.9	74.7
	K	17.9	18.0	13.9	16.1	19.8	18.8	18.7	16.5	15.3	18.3	21.1	14.3
	P	11.9	10.0	8.1	6.9	9.5	12.0	9.8	7.9	10.2	10.1	10.0	11.0
	Qmr	47.8	64.3	64.3	70.0	57.4	61.3	64.0	62.0	53.5	50.0	61.2	63.7
	Qmo	22.7	20.0	21.7	20.4	16.6	19.7	18.7	19.0	19.7	25.0	20.2	20.7
	Qp	29.6	15.7	14.0	9.6	26.0	19.0	17.3	19.0	26.8	25.0	18.6	15.6
	Rg/Rt	0.60	0.63	1.00	1.00	0.61	0.78	0.75	0.70	0.50	0.60	0.50	1.00
	F/Qm	0.42	0.39	0.28	0.30	0.41	0.44	0.40	0.32	0.34	0.40	0.45	0.34
	P/F	0.40	0.36	0.37	0.30	0.32	0.39	0.34	0.32	0.40	0.35	0.32	0.44

Table 2. (Continued)

		Puerto a Coruña								
		PTC-51,45	PTC-45,1	PTC-44,3	PTC-42,60	PTC2-40,8	PTC-40,40	PTC-39,00	PTC2-37,8	PTC-35,80
AN										
Q										
Qmr	Monocrystalline non-undulose quartz	151	152	177	202	102	96	115	150	116
Qmo	Monocrystalline undulose quartz	31	51	34	62	9	34	33	17	21
Qp2-3	Polycrystalline quartz (2-3 crystals)	7	12	10	18	4	9	12	10	11
Qp>3	Polycrystalline quartz (>3 crystals)	4	16	2	3	1	18	11	1	9
Qrm	Quartz in low and medium meta. grade rock fragm.									
Qrp	Quartz in plutonic rock fragment		1			3	4		2	2
Qrg	Quartz in gneissic rock fragment									1
Qrs	Quartz in sandstone									
K										
Ks	K-feldspar (single crystal)	14	24	22	7	96	43	25	46	30
Krm	K-feldspar in low and medium meta. grade rock fragm.									
Krp	K-feldspar in plutonic rock fragment		1			8	3			3
Krg	K-feldspar in gneissic rock fragment									
P										
Ps	Plagioclase (single crystal)	9	8	17	6	81	31	29	36	21
Prm	Plagioclase in low and medium meta. grade rock fragm.									
Prp	Plagioclase in plutonic rock fragment									
M										
Bi	Biotite (single crystal)	1				23	9	4	7	
Mu	Muscovite (single crystal)					35	8	6	9	4
Cl	Chlorite (single crystal)							1		1
Mrm	Mica in low and medium meta. grade rock fragm.									
L										
Ch	Unspecified chert			1	3	2				
Sh	Shale and fillites	2	2	2			4			3
Dm	Dense minerals (unspecified)		1	1	1	4	4	5	3	
MC										
	Molusc						34	15	6	67
	Echinoderm								1	
	Foram.; red algae; briozoo.; ostracods						3	2	5	7
	Indeterminate bioclast						18	17	32	20
MN										
	Silty-clay soft grains, glauconite	116	40	37	1	4	9	32	1	
	Fe-Oxides, alterite	18			1	3	8	11	1	5
	Total	353	308	303	304	378	335	319	327	321
	MC/T	0.00	0.00	0.00	0.00	0.00	0.16	0.11	0.13	0.29
	AN/T	0.62	0.87	0.88	0.99	0.98	0.79	0.76	0.86	0.69
	Q	88.5	86.5	84.5	95.7	38.2	64.9	75.7	67.9	72.4
	F	10.6	12.0	14.7	4.3	57.3	30.6	23.9	31.3	23.5
	R	0.9	1.5	1.1	1.0	5.2	4.5	0.4	0.8	4.1
	Qm	88.5	86.9	84.2	94.7	38.5	66.5	75.7	68.7	73.7
	F	10.6	12.4	14.7	4.3	60.8	31.8	24.3	31.3	24.9
	Lt	0.9	0.7	1.1	1.0	0.6	1.7	0.0	0.0	1.4
	Qm	89.4	87.5	85.1	95.6	38.8	67.6	75.7	68.7	74.8
	K	6.5	9.4	8.4	2.3	33.9	19.3	11.1	17.6	15.4
	P	4.2	3.0	6.5	2.0	27.4	13.0	13.3	13.7	9.8
	Qmr	78.2	65.8	79.4	70.9	87.9	61.1	67.3	84.3	73.9
	Qmo	16.1	22.1	15.2	21.8	7.8	21.7	19.3	9.6	13.4
	Qp	5.7	12.1	5.4	7.4	4.3	17.2	13.5	6.2	12.7
	Rg/Rt	0.00	0.50	0.00	0.00	0.88	0.64	1.00	1.00	0.67
	F/Qm	0.12	0.14	0.17	0.05	1.58	0.48	0.32	0.46	0.34
	P/F	0.39	0.24	0.44	0.46	0.45	0.40	0.55	0.44	0.39

(Continued)

Table 2. (Continued)

		Miño									
		MIÑ-21,85	MIÑ-14,4	MIÑ-12,8	MIÑ-10,6	MIÑ-9,2	MIÑ-7,1	MIÑ-5,6	MIÑ-4,5	MIÑ-2,8	MIÑ-2,0
AN											
Q											
Qmr	Monocrystalline non-undulose quartz	130	179	117	157	174	136	161	145	172	148
Qmo	Monocrystalline undulose quartz	21	43	15	36	23	42	49	43	52	49
Qp2-3	Polycrystalline quartz (2-3 crystals)	10	5	19	12	10	11	8	15	11	13
Qp>3	Polycrystalline quartz (>3 crystals)	7	12	27	7	4	9	11	8	10	7
Qrm	Quartz in low and medium meta. grade rock fragm.	1		3	1				3		
Qrp	Quartz in plutonic rock fragment	1	1	5	1	2	2	1	1	2	1
Qrg	Quartz in gneissic rock fragment										
Qrs	Quartz in sandstone										
K											
Ks	K-feldspar (single crystal)	15	29	36	47	31	44	35	35	23	29
Krm	K-feldspar in low and medium meta. grade rock fragm.										
Krp	K-feldspar in plutonic rock fragment	1		5	3		1		1	1	1
Krg	K-feldspar in gneissic rock fragment										
P											
Ps	Plagioclase (single crystal)	16	27	30	25	26	44	22	23	22	34
Prm	Plagioclase in low and medium meta. grade rock fragm.										
Prp	Plagioclase in plutonic rock fragment			2	2	1	1			1	1
M											
Bi	Biotite (single crystal)	67		17	5			3	2		3
Mu	Muscovite (single crystal)	23	2	29	4	1		2			3
Cl	Chlorite (single crystal)	15									
Mrm	Mica in low and medium meta. grade rock fragm.	1	1	4	2						1
L											
Ch	Unspecified chert	3			1						
Sh	Shale and fillites	3		7	3				4	2	
Dm	Dense minerals (unspecified)	6	5	9	7	9	3	4	9	10	14
MC											
	Molusc					6		1	8		
	Echinoderm					1	1	2	2		
	Foram.; red algae; briozoo.; ostracods						10		3		
	Indeterminate bioclast					16		7	12		
MN											
	Silty-clay soft grains, glauconite				1	0		1	0		0
	Fe-Oxides, alterite				1						
	Total	320	304	325	315	304	304	307	314	306	304
	MC/T	0.00	0.00	0.00	0.00	0.08	0.04	0.03	0.08	0.00	0.00
	AN/T	1.00	1.00	1.00	0.99	0.92	0.96	0.96	0.92	1.00	1.00
	Q	81.8	80.5	65.9	71.7	77.9	68.3	79.8	75.9	82.8	76.4
	F	14.8	18.9	24.4	24.2	21.0	30.3	19.9	20.9	15.2	22.2
	R	4.8	0.7	9.6	4.4	1.1	1.4	0.3	3.2	2.0	1.4
	Qm	81.7	81.1	69.9	72.5	78.6	69.0	80.1	77.3	83.4	77.0
	F	15.4	18.9	27.4	26.1	21.4	31.0	19.9	21.2	15.9	23.0
	Lt	2.9	0.0	2.6	1.4	0.0	0.0	0.0	1.4	0.7	0.0
	Qm	84.2	81.1	71.8	73.5	78.6	69.0	80.1	78.5	84.0	77.0
	K	7.9	9.8	15.8	17.2	11.4	15.5	12.2	13.1	8.2	10.6
	P	7.9	9.1	12.4	9.3	10.0	15.5	7.7	8.4	7.8	12.4
	Qmr	77.4	74.9	65.7	74.1	82.5	68.7	70.3	68.7	70.2	68.2
	Qmo	12.5	18.0	8.4	17.0	10.9	21.2	21.4	20.4	21.2	22.6
	Qp	10.1	7.1	25.8	9.0	6.6	10.1	8.3	10.9	8.6	9.2
	Rg/Rt	0.20	0.50	0.46	0.46	1.00	1.00	1.00	0.22	0.67	0.75
	F/Qm	0.19	0.23	0.39	0.36	0.27	0.45	0.25	0.27	0.19	0.30
	P/F	0.50	0.48	0.44	0.35	0.47	0.50	0.39	0.39	0.49	0.54

Table 2. (Continued)

		Pantín									
		PAN-16,6	PAN-14,7	PAN-12,7	PAN-11,2	PAN-10,4	PAN-8,6	PAN-6,6	PAN-4,6	PAN-2,6	PAN-1,5
AN											
Q											
Qmr	Monocrystalline non-undulose quartz	135	164	127	154	149	154	121	141	128	127
Qmo	Monocrystalline undulose quartz	24	31	23	44	36	40	27	40	25	37
Qp2-3	Polycrystalline quartz (2-3 crystals)	15	7	9	11	14	10	4	10	15	14
Qp>3	Polycrystalline quartz (>3 crystals)	11	11	17	13	9	8	15	20	28	32
Qrm	Quartz in low and medium meta. grade rock fragm.	2	2						2	2	2
Qrp	Quartz in plutonic rock fragment			2	1		1		3	2	1
Qrg	Quartz in gneissic rock fragment										
Qrs	Quartz in sandstone										
K											
Ks	K-feldspar (single crystal)	16	16	19	23	22	14	22	22	37	29
Krm	K-feldspar in low and medium meta. grade rock fragm.			1	1		2				1
Krp	K-feldspar in plutonic rock fragment		1						2		1
Krg	K-feldspar in gneissic rock fragment										
P											
Ps	Plagioclase (single crystal)	10	11	18	10	14	15	15	15	16	22
Prm	Plagioclase in low and medium meta. grade rock fragm.	1							1		
Prp	Plagioclase in plutonic rock fragment						1		1	1	
M											
Bi	Biotite (single crystal)										
Mu	Muscovite (single crystal)	4	2						1		1
Cl	Chlorite (single crystal)										
Mrm	Mica in low and medium meta. grade rock fragm.			1	1				1	2	
L											
Ch	Unspecified chert										
Sh	Shale and fillites	2	1	2				1	2	2	3
Dm	Dense minerals (unspecified)	6	14	9	18	10	10	9	9	19	13
MC											
	Molusc	53	18	38	14	23	18	26	17	16	14
	Echinoderm	5	4	3		3	4	5	4	1	1
	Foram.; red algae; briozoo.; ostracods	3	1								
	Indeterminate bioclast	27	24	37	13	20	27	56	22	15	11
MN											
	Silty-clay soft grains, glauconite Fe-Oxides, alterite										
	Total	314	307	306	303	300	304	302	313	309	308
	MC/T	0.28	0.15	0.25	0.09	0.15	0.16	0.29	0.14	0.10	0.08
	AN/T	0.72	0.85	0.75	0.91	0.85	0.84	0.71	0.86	0.90	0.92
	Q	85.6	87.3	80.4	86.0	85.2	86.5	81.5	81.2	76.3	78.1
	F	12.0	11.1	16.9	12.8	14.8	11.8	18.0	14.2	20.6	19.0
	R	2.3	1.6	2.7	1.2	0.0	1.6	0.5	4.6	3.1	3.0
	Qm	86.6	88.1	81.7	86.8	85.2	86.9	81.5	83.4	78.4	79.2
	F	12.5	11.5	17.4	13.2	14.8	13.1	18.0	15.8	20.8	19.7
	Lt	0.9	0.4	0.9	0.0	0.0	0.0	0.5	0.8	0.8	1.1
	Qm	87.4	88.5	82.4	86.8	85.2	86.9	81.9	84.0	79.1	80.1
	K	7.5	7.0	9.3	9.3	9.0	6.5	10.8	9.3	14.6	11.7
	P	5.1	4.5	8.3	3.9	5.7	6.5	7.4	6.6	6.3	8.3
	Qmr	73.0	77.0	72.2	69.4	71.6	72.6	72.5	66.8	65.3	60.5
	Qmo	13.0	14.6	13.1	19.8	17.3	18.9	16.2	19.0	12.8	17.6
	Qp	14.1	8.5	14.8	10.8	11.1	8.5	11.4	14.2	21.9	21.9
	Rg/Rt	0.20	0.25	0.33	0.33	–	0.50	0.00	0.50	0.25	0.25
	F/Qm	0.14	0.13	0.21	0.15	0.17	0.15	0.22	0.19	0.27	0.25
	P/F	0.41	0.39	0.47	0.29	0.39	0.50	0.41	0.41	0.30	0.42

(Continued)

Table 2. (Continued)

		Vivero - Pte.					Vivero - Ind.					Navia		
		E2-9-23,5	E2-5-12,75	E2-4-10,5	E2-2-6	E2-1-4	VIV-I-3,6	VIV-I-2,85	VIV-I-2,75	VIV-I-2,45	VIV-I-1,5	NAV-19,2	NAV-17,6	NAV-16,8
AN														
Q														
Qmr	Monocrystalline non-undulose quartz	108	134	116	110	146	132	135	132	130	153	79	150	39
Qmo	Monocrystalline undulose quartz	18	31	10	37	23	21	22	19	24	38	43	43	23
Qp2-3	Polycrystalline quartz (2-3 crystals)	8	13	10	16	13	10	8	12	12	13	24	23	12
Qp>3	Polycrystalline quartz (>3 crystals)	5	7	11	7	7	16	8	13	6	6	22	18	19
Qrm	Quartz in low and medium meta. grade rock fragm.	2	2		1		1		1			6	6	3
Qrp	Quartz in plutonic rock fragment	7	2	5	5	2	6	6	6	5	5			
Qrg	Quartz in gneissic rock fragment													
Qrs	Quartz in sandstone													4
K														
Ks	K-feldspar (single crystal)	74	43	61	64	81	56	59	51	57	42	8	12	6
Krm	K-feldspar in low and medium meta. grade rock fragm.											2		
Krp	K-feldspar in plutonic rock fragment	2	4	6	2	4	3	2	4	7	2		1	
Krg	K-feldspar in gneissic rock fragment													
P														
Ps	Plagioclase (single crystal)	29	28	17	39	23	17	19	24	19	18	4	4	5
Prm	Plagioclase in low and medium meta. grade rock fragm.													
Prp	Plagioclase in plutonic rock fragment	2	2	1	1	1	3	2	4	3			1	
M														
Bi	Biotite (single crystal)	38	1	8	20	1	10	10	12	7	9			
Mu	Muscovite (single crystal)	18	3	13	13	5	14	14	19	5	6	8	6	4
Cl	Chlorite (single crystal)													
Mrm	Mica in low and medium meta. grade rock fragm.	11		2	2		1	3	3	1	3	1	3	
L														
Ch	Unspecified chert													
Sh	Shale and fillites	10	2	3	11	1	3	3	4	4	5	30	47	20
Dm	Dense minerals (unspecified)	17	9	11	7	5	1	5	7	4	3	5	8	2
MC														
	Molusc	1	16	30			14	17	10	18	6	16		58
	Echinoderm		10	7			6	4	1	2	1	10		12
	Foram.; red algae; briozoo.; ostracods			2			2	2	3	1		43		46
	Indeterminate bioclast	1	17	24		1	10	18	26	26	15	21		76
MN														
	Silty-clay soft grains, glauconite Fe-Oxides, alterite		1						1	1		1	3	
	Total	351	325	337	335	313	326	337	351	332	325	323	325	329
	MC/T	0.01	0.13	0.19	0.00	0.00	0.10	0.12	0.11	0.14	0.07	0.28	0.00	0.58
	AN/T	0.99	0.86	0.81	1.00	1.00	0.90	0.88	0.89	0.86	0.93	0.72	0.99	0.42
	Q	50.4	69.0	60.7	57.6	62.8	66.5	64.8	64.5	64.2	73.7	76.7	76.0	71.0
	F	37.3	26.5	32.2	34.9	34.6	27.1	29.2	27.5	28.4	21.1	5.5	5.2	8.4
	R	12.3	4.5	7.0	7.5	2.7	6.3	6.0	8.1	7.5	5.3	17.8	18.8	20.6
	Qm	55.8	70.5	63.3	60.1	63.5	69.4	67.8	67.8	66.3	76.2	79.8	78.7	76.3
	F	40.4	28.7	35.4	36.2	36.2	29.5	31.1	30.7	32.2	22.0	6.4	5.9	8.4
	Lt	3.8	0.7	1.3	3.8	0.3	1.1	1.1	1.5	1.5	1.8	13.8	15.4	15.3

Table 2. (Continued)

	Vivero - Pte.					Vivero - Ind.					Navia		
	E2-9-23,5	E2-5-12,75	E2-4-10,5	E2-2-6	E2-1-4	VIV-I-3,6	VIV-I-2,85	VIV-I-2,75	VIV-I-2,45	VIV-I-1,5	NAV-19,2	NAV-17,6	NAV-16,8
Qm	58.0	71.1	64.1	62.4	63.7	70.2	68.6	68.8	67.3	77.6	92.6	93.0	90.1
K	29.8	17.7	28.3	23.4	28.3	22.3	23.4	20.7	24.3	15.9	5.3	5.0	5.4
P	12.2	11.3	7.6	14.2	8.0	7.5	8.0	10.5	8.4	6.5	2.1	1.9	4.5
Qmr	77.7	72.4	78.9	64.7	77.2	73.7	78.0	75.0	75.6	72.9	47.0	64.1	41.9
Qmo	12.9	16.8	6.8	21.8	12.2	11.7	12.7	10.8	14.0	18.1	25.6	18.4	24.7
Qp	9.4	10.8	14.3	13.5	10.6	14.5	9.2	14.2	10.5	9.0	27.4	17.5	33.3
Rg/Rt	0.32	0.67	0.71	0.36	0.88	0.71	0.63	0.64	0.75	0.47	0.00	0.03	0.00
F/Qm	0.72	0.41	0.56	0.60	0.57	0.42	0.46	0.45	0.49	0.29	0.08	0.08	0.11
P/F	0.29	0.39	0.21	0.38	0.22	0.25	0.26	0.34	0.26	0.29	0.29	0.28	0.45

The main composition of sands in the Navia Holocene record differs drastically from that of the Galician coast. These sands constitute a quartzolithic petrofacies with greater contents of rock fragments (18–20% R) than feldspars (5–8%). This composition also reflects the sedimentary and low-grade metamorphic nature of their source areas (WALZ ofthe Iberian Massif). No differences exist in the Navia QFR and QmFLt diagrams, suggesting that rock fragments in these sands are shales and other fine-grained lithic components.

Sand from the Galician Holocene record shows a homogeneous distribution of their composition in the QFR and QmFLt diagrams (Figure 3). However, it is also clear that the composition of sand from each location constitutes an individual cluster related to characteristics of the given source area. Sands from Vivero (Puente and Indiano) show the largest amount of feldspars, and are associated with abundant granitoids in their sources (Table 1). In contrast, sands from Pantín are the most quartzose and are related to the lowest occurrence of granitoids in their sources (Table 1). In other locations (Pto. Coruña and Miño), feldspar contents vary through the stratigraphic record. These variations could be associated with mixing processes between fluvial sands and sands of a marine origin.

In spite of the quartzofeldspathic character of the Galician Holocene sands, fine-grained lithic fragments (shales and phyllites) are also present. These components appear in low percentages (<4%) at the sites where these sedimentary and low-grade metamorphic rocks are abundantly represented in their sources, such as at Vivero, Pto. Coruña and Miño. This under-representation of such sources in sands is due to the great potential of granitoids to produce sand (Sand Generation Index of Palomares and Arribas, 1993), intensely diluting supplies from metasedimentary lithologies.

Quartzofeldspathic composition of Holocene Galician sands is consistent with the composition of other sands of the western coast of the Iberian Peninsula (Marsaglia *et al.*, 1996, 2007; Le Pera and Arribas, 2005).

Feldspar composition (QmKP)

The feldspar grain population is dominated by K-feldspars (P/F 0.5 to 0.21, Table 2). Monocrystalline untwinned albite grains are also present and occur in association with twinned plagioclase grains. Samples with higher contents of plagioclase grains are mainly those from Miño, Pto. Coruña and Pantín (P/F>0.4), where amphibolites are the source rocks. Samples from Vivero (Puente and Indiano sites) have greater K-feldspar contents (mean P/F<0.3). Petrographic relations between K and P grains could be correlated with the lithology and characteristics of granitoids and related metamorphic rocks as the sources of sand (sea cliffs and drainage basins). Analyses performed on Galician granitic rocks (Cuesta, 1991) indicate a mean modal composition close to $Q_{30}K_{40}P_{30}$. Thus, the P/F ratios obtained in Holocene sand samples are in line with the mean P/F ratio for granites. Local fluctuations in this ratio in sands can be explained by additional supplies from other mafic lithologies (e.g. amphibolites) or by maturation processes during transport.

The Holocene Galician sands mainly plot above the 65% Qm line in the QmKP ternary diagram (Figure 4a). This suggests their high compositional maturity, compared with the modal composition of Galician granitoids or other pure plutoniclastic sands (figure 10 in Le Pera *et al.*, 2001). In addition, plots for Holocene sands from each locality exhibit a line distribution with near constant P/F values, while Qm contents increase (Figure 4a). These plots suggest no significant processes of differential loss between the two types of feldspar, as both disappear simultaneously during quartz enrichment, and thus during sand maturation. This sort of process can be related to mechanical abrasion in coastal environments (e.g. Le Pera and Arribas, 2005; Fillali *et al.*, 2005).

Rock fragments

Rock fragments occur in low proportion because of the dominance of monomineral clasts from plutonites. They include coarse crystalline rock fragments and some fine-grained metamorphic rocks.

The relative proportions of coarse crystalline rock fragments (Rg) versus the total population of rock fragments (Rt=Rg+Rm) in sands from all the sites are provided in Figure 5. Sands from Traba and Navia show the two extremes of the distribution of total sands, suggesting the monolithologic nature of their sources. At the Traba site, the lithic population is entirely composed of coarse-grained rock fragments, while fine-grained rocks predominate at the Navia site. The nature of the lithic population of each location varies with shifts to the right or left area of the diagram. Locations with consistent coarse-grained lithologies (granitoids) in their sources (Vivero and Baldaio) plot in the area to the right. Sands from locations in which fine-grained rocks predominate (Pantín), plot to the left. Sands from Miño and Pto.

Table 3. Sedimentary environments, ages and sand textures (grain size, sorting and quartz roundness) inferred from the Holocene records examined

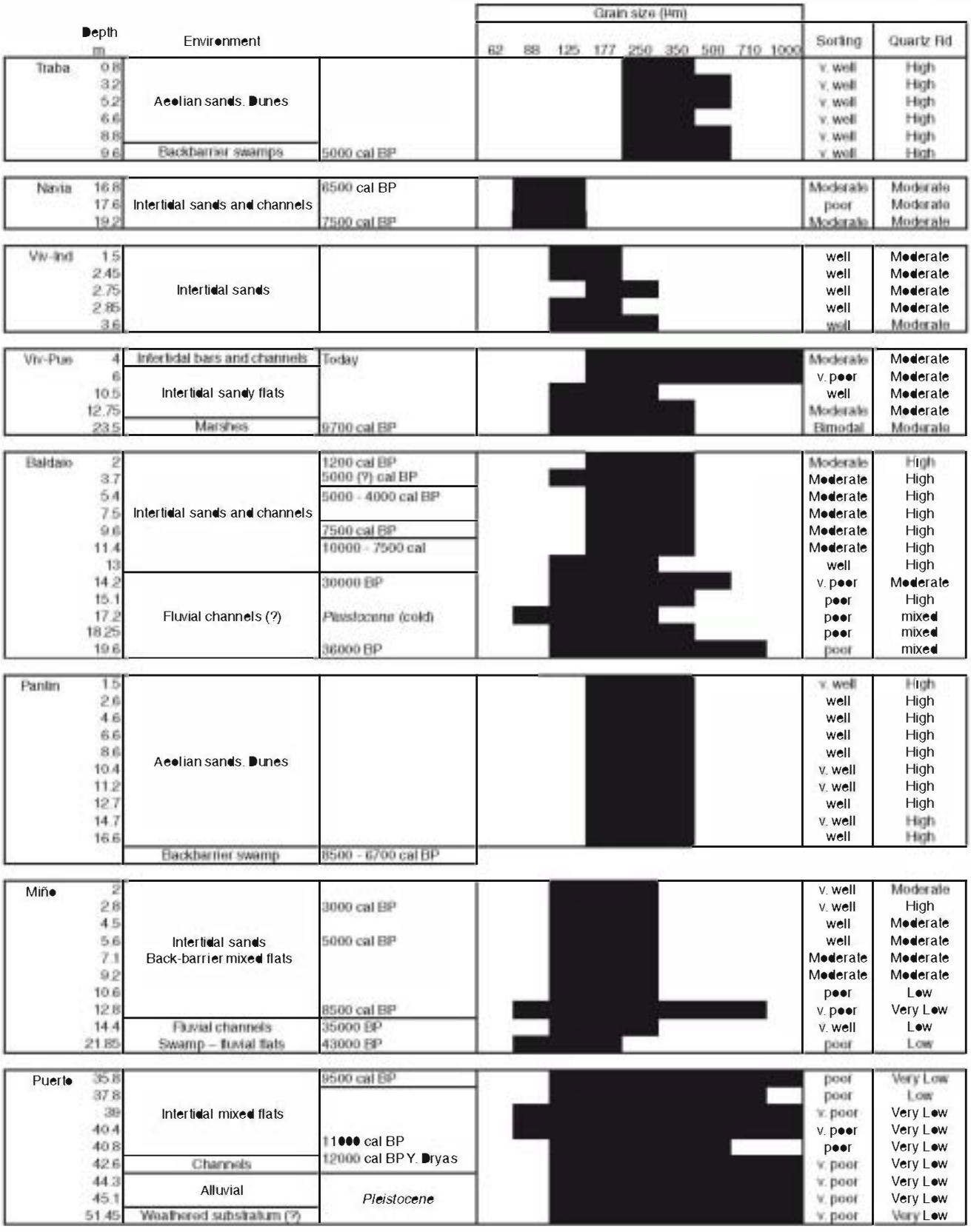

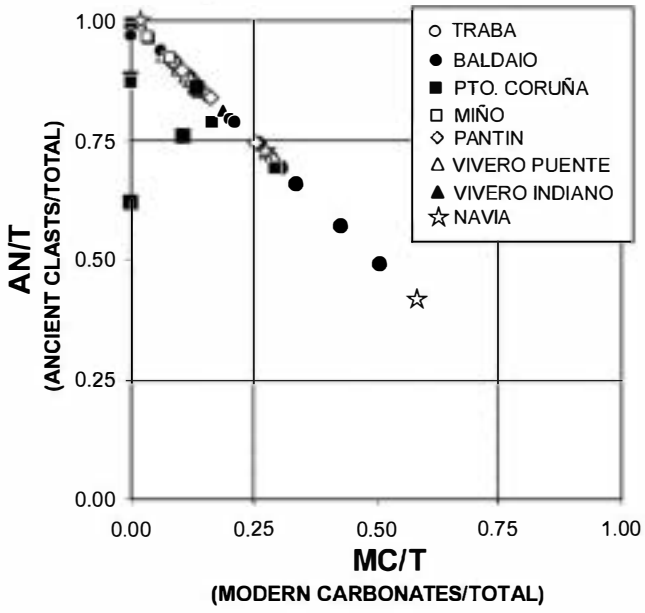

Figure 2. MC/T versus AN/T binary diagram (modified from Di Giulio and Valloni, 1992) showing the composition of the Holocene sands examined

Coruña show highly variable lithic nature, with fluvial sands showing the greatest abundance of fine-grained rock fragments (Figure 5 and Table 2).

Quartz grain typologies

Monocrystalline is the main quartz grain typology of the analysed sands (Figure 6), with a predominance of the non-undulose variety (Qmr). Sands from Vivero, Pantín, Miño and Pto. Coruña show the highest contents of this quartz grain type. In contrast, sands from Traba have greater proportions of the undulose variety (Qmo). The predominance of monocrystalline typologies can be related to their origin, associated with coarse-grained plutonites, mainly granitoids (Basu *et al.*, 1975; Tortosa, 1988; Tortosa *et al.*, 1991; Heins, 1993). Differences between undulose and non-undulose types may suggest differences in deformation of the original source rock (e.g. Tortosa *et al.*, 1991). In addition, the population of monocrystalline non-undulose quartz grains may be increased by supplies from sedimentary sources (Blatt *et al.*, 1980; Arribas and Tortosa, 2003).

Polycrystalline quartz grain typologies are also present. Sands from the Navia, Baldaio and Pantín records exhibit the highest amounts of polycrystalline quartz grains (Figure 6), but with percentages of 15 to 35% of total quartz. The presence of these types is related to fine-grained metamorphic sources (Basu *et al.*, 1975; Tortosa *et al.*, 1991). The great drainage basin of Navia is mainly composed of sedimentary and metasedimentary rocks from the Western Asturian Leonese Zone of the Iberian Massif, and thus, the proportion of quartz types in sands is consistent with the composition of their sources (Table 1). The relatively high contents of polycrystalline types in the Baldaio and Pantín sands could be related to the presence of schists and paragneiss in their near sources (Bastida *et al.*, 1984; González Lodeiro *et al.*,1984). In other localities, the presence of fine-grained metamorphic rocks does not lead to large quantities of polycrystalline quartz types in their derived sands (e.g. Vivero), suggesting dilution of these supplies by plutoniclastic sands derived from granitoids in the same

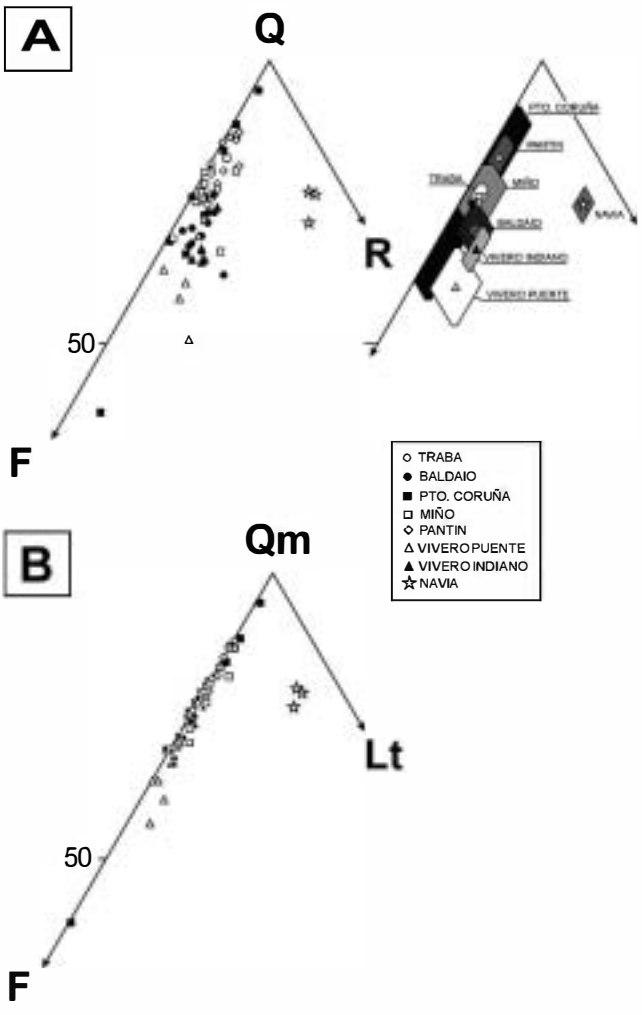

Figure 3. (A) Holocene sand compositions represented in a QFR diagram (Pettijohn *et al.*, 1972). Polygons in the inset diagram provide the means and standard deviations obtained for samples grouped by deposition site. (B) Holocene sand compositions represented in a QmFLt diagram (Dickinson *et al.*, 1983)

source, or alternatively, their downstream mechanical destruction during transport (e.g. Cameron and Blatt, 1971; Mack, 1978).

Discussion

Environments, sand textures and composition of modern clasts

As mentioned in the above sections, the textures of Holocene sands are highly dependent on several mechanical processes acting on specific environments. Hydrodynamic and aeolian sorting produces narrow grain-size intervals in intertidal and dune environments (mainly 177 to 350 μm), generating well- and very well-sorted grain populations, respectively. Intense mechanical abrasion in dunes leads to high quartz roundness; in intertidal deposits, quartz roundness is moderate. An intense contrast exists with fluviatile sand deposits (channel fills and marshes). These last populations show wider grain-size intervals with common coarser clasts and poorly sorted deposits with scarcely rounded quartz grains. Locally, the presence of embayed quartz grains reveals the development of soil profiles in fluvial drainage basins (Cleary and Conolly, 1971).

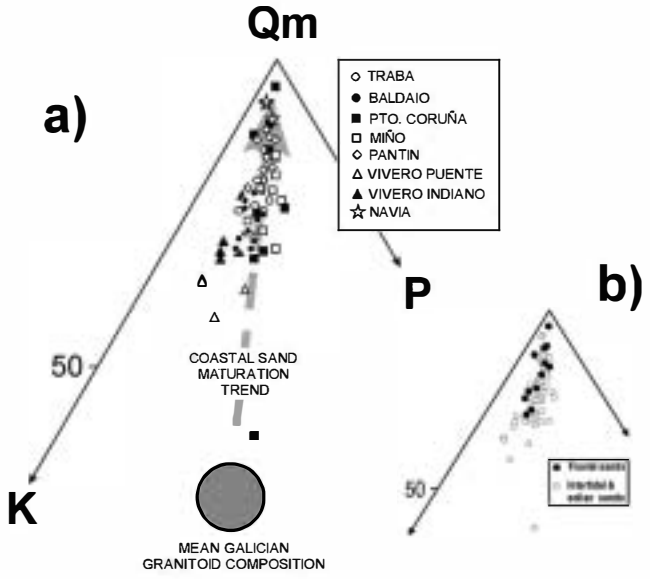

Figure 4. (a) Holocene sand compositions represented in a QmKP diagram (Dickinson *et al.*, 1983). Also plotted are mean Galician granitoid compositions obtained from data in Cuesta (1991). (b) Similar diagram to (a) in which fluvial sands are discriminated from coastal sands

In addition, the presence of several modern non-carbonate grain types (MN), such as alterites, Fe-oxides and silty-clayey soft grains, characterizes fluviatile deposits and highlights the land-derived nature of these sands. In contrast, the occurrence of modern carbonate grains (MC) is correlated with sands from marine sources. In intertidal deposits, the amount of MC fluctuates (e.g. Baldaio, Pto. Coruña), but in aeolian sands, this amount is nearly constant through the Holocene record (e.g. Traba, Pantín) (see Figure 7). This could be due to a homogenization process of aeolian deposits due to reworking and incorporation of intertidal sands in the aeolian environment (e.g. Cann *et al.*, 1999; Clemmensen *et al.*, 2001; Pease and Tchakerian, 2002). However, at some sites (Pto. Coruña and Baldaio), MC grains increase toward the top of the Holocene sequence, suggesting the progressive influence of marine supplies.

Source lithology and sand composition

The main modal composition of Galician Holocene sands reflects a homogeneous mature quartzofeldspathic petrofacies contrasting with the quartzolithic petrofacies of the Navia sands. In both cases, the main control on sand composition is the source lithology: dominance of coarse granitoids from the GTMZ and gneisses from the CIZ for the Galician sands, and dominance of metasedimentary rocks from the Asturian Leonese Zone for the Navia sands (Figure 3 and Table 1).

Despite the homogeneous composition of the Galician sands, differences among individual locations exist. These differences reflect variations in local source rock. Aeolian sands and those generated in areas with small drainage basins show more restricted clusters (Traba, Pantín and Baldaio), while locations with more developed drainage basins display more variable sand composition (Pto. Coruña, Miño and Vivero). These features are confirmed in the QFR, QmFLt, QmKP and Rg/Rt diagrams (Figures 3, 4 and 5), and suggest processes such as mixing and maturation during transport acting mainly on the larger fluvial drainage basins. An exception is the great drainage basin of Navia, which gives rise to sands of similar composition. This finding can be attributed to the monotonous lithological nature of the Navia drainage basin (metasedimentary rocks), which is unable to produce consistent variations in the composition of its sandy products by maturation during transport.

It is also clear that the presence of coarse-grained source rocks generates large quantities of monomineral grains (quartz and feldspar), diluting supplies from other parent rocks of lower SGI such as schists or metasediments (Palomares and Arribas, 1993). The

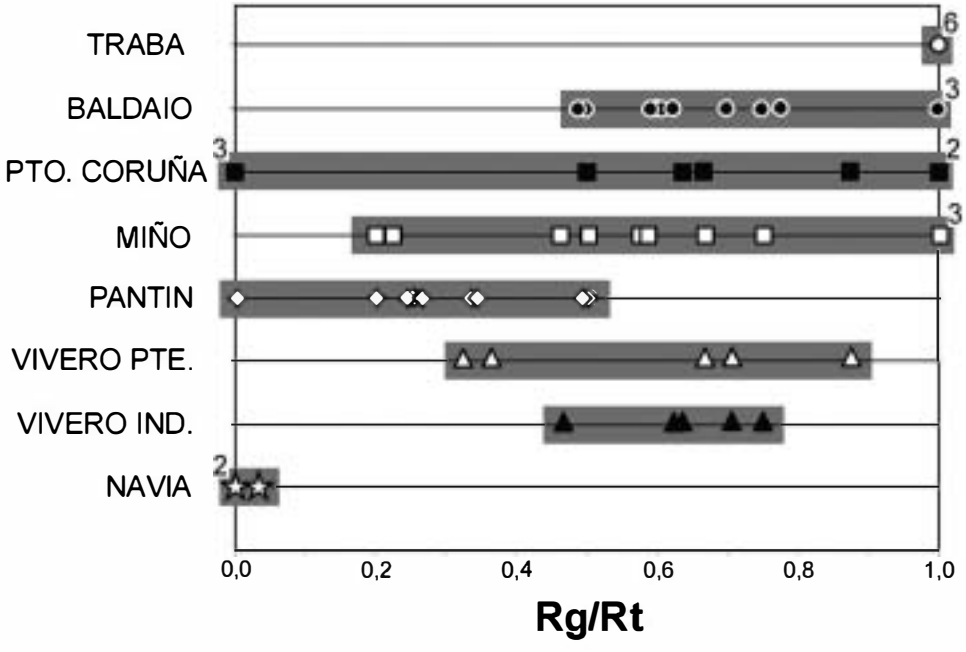

Figure 5. Rg/Rt ratios (coarse grained rock fragments / total rock fragments) determined in the Holocene sands grouped by deposition site

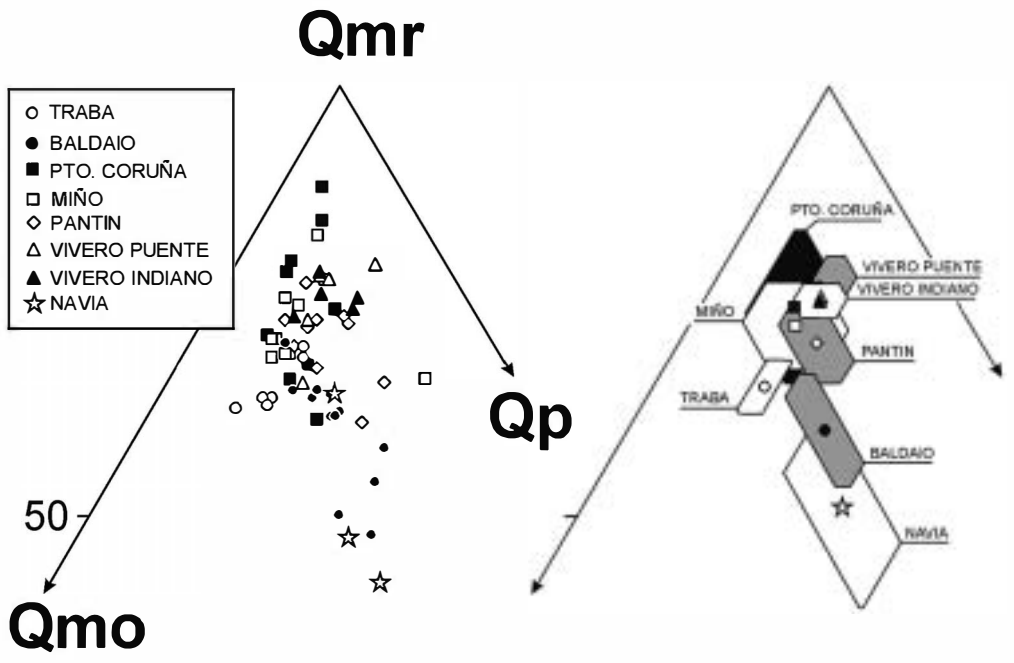

Figure 6. Distribution of quartz typologies in the Holocene sands (Qmr, monocrystalline quartz; Qmo, monocrystalline non-undulatory quartz; Qp, pollycrystalline quartz). Polygons in the inset diagram show the means and standard deviations of samples grouped by deposition site

identification of these under-represented source rocks in sands is difficult, the Rg/Rt diagram being a very useful tool for this purpose. In addition, quartz typologies may help discriminate deformed (e.g. Traba) from non-deformed (i.e. Pantín) granitoids at the sources (Qmr versus Qmo types), and to identify supplies from fine-grained metamorphic rocks (i.e. Navia, Baldaio) with greater Qp/Qm values.

Evolving sand composition: fluvial versus marine supplies

Changes in sand composition produced during Holocene deposition can be analysed through variations in petrographic indices such as carbonate clasts to total clasts, MC/T; feldspars to monocrystalline quartz, F/Qm; and plagioclase to total feldspars, P/F (Figure 7). Most significant variations in composition are reflected by the MC/T index, which is related to changes in the sedimentary environment.

Aeolian sands (Traba and Pantín) show trends of near constant values in their F/Qm: 0.3 and 0.2, respectively. These constant records are consistent with the homogenization process that affects aeolian sands, discussed above. A more variable trend in F/Qm was recorded for Baldaio, with values close to 0.4. Fluvial and intertidal sands at this location show good fit with the MC/T index, suggesting the better preservation of feldspars in sands with greater marine supplies. Maxima of both indices have been recorded at depths of 3.7 m (5000 BP) and 13 m (10 000 BP) and could be related to important transgressive events. In other sites, F/Qm values are highly variable, as occurs in the Pto. Coruña and Miño records. In these places, a rougher fitting to MC/T exists, and fluvial sands are those showing greater quartz enrichment. Among the trends shown by Vivero and Navia, we find that in few samples did petrographic indices show high variation; thus, no consistent pattern can be inferred for these localities.

Trends in P/F exhibit similar variation, mainly from 0.3 to 0.5. Navia and Vivero are the sites showing more enrichment in K-feldspar sands (P/F<0.4), while the Miño sands and sands from the upper part of Pto. Coruña section include the highest P/F (>0.4). These data are related to the source lithology and the absence (i.e. Vivero) or presence (i.e. Miño, Pto. Coruña) of mafic rocks (i.e. amphibolites) accompanying the main granitic sources. These basic sources provide plagioclase-enriched sands, with higher P/F. Many sands with maximum P/F in their local trend concur with maximum F/Qm values, suggesting good conditions for feldspar preservation, even for the more unstable feldspars such as plagioclase. These sands occur at depths of 13 m in Baldaio; 7.1 m in Miño; and 12.7 m in Pantín, and might be correlated with transgressive events.

It may be concluded that sands from each location show an individual composition that may change over time but is always within a given range. This suggests that long-distance transport of marine sand can be disregarded. Thus, the irregular Galician coast produces short-distance transport from western areas and deposition on sediment-trap sites.

Weathering of land sources and provenance of supplies

The presence of embayed quartz and alterite grains suggests weathering processes acting on drainage basins. In addition, the most mature sands represent fluvial supplies at the Pto. Coruña and Miño localities, and significant changes in composition occur where intertidal deposits occur. As a whole, fluvial sands are more mature in their QmKP composition than intertidal/aeolian sands (Figure 4b), with greater Qm contents (more than 70%) and lower values of P (less than 12%). This means that marine deposits cannot be considered simply as products reworked from fluvial deposits. Thus, there must be substantial differences in the origin of sands between fluvial and marine deposits.

Nesbitt *et al.* (1997) demonstrated that weathering processes in soils produce severe reduction in plagioclase sand grains.

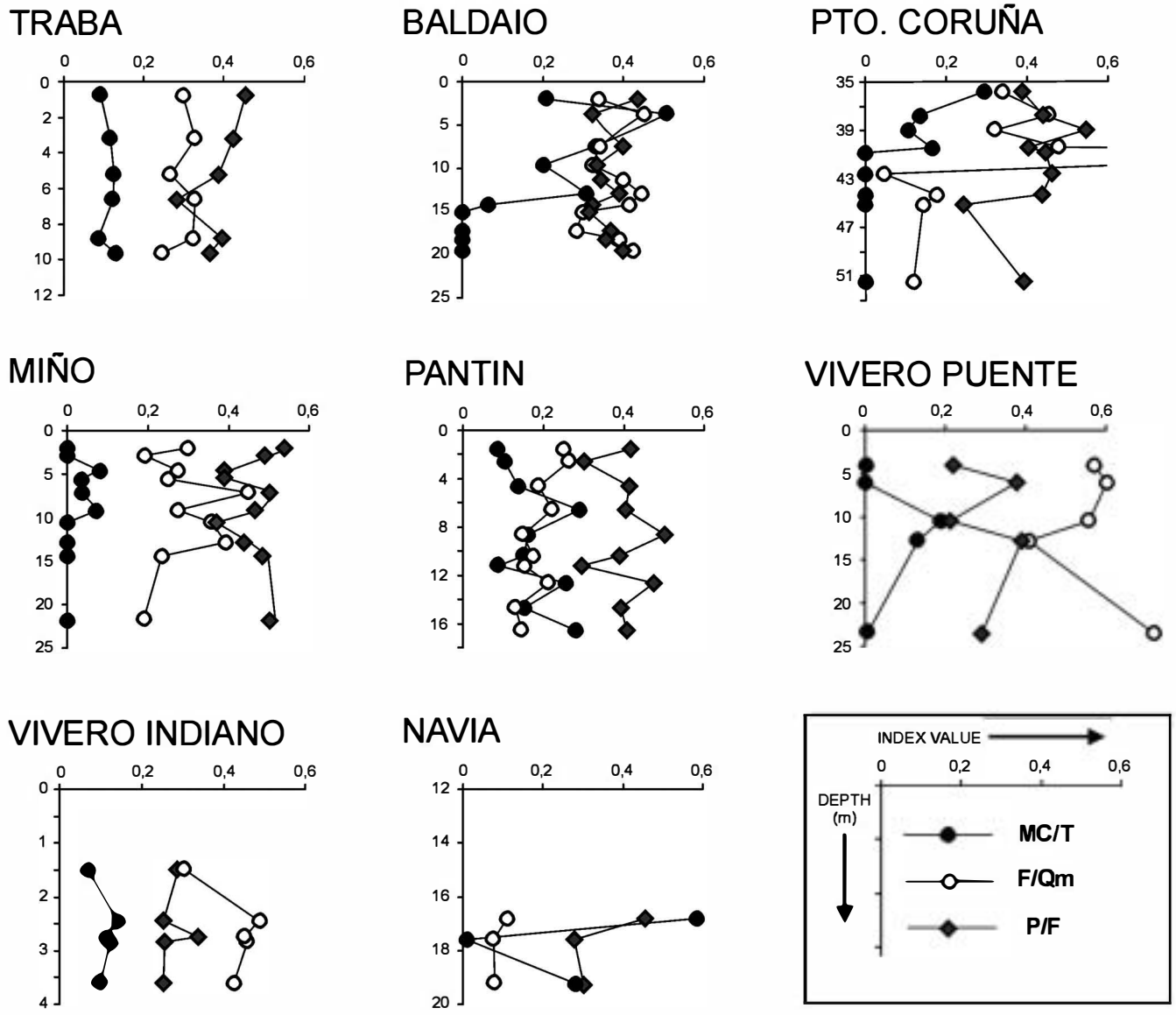

Figure 7. Variations in MC/T (modern carbonates/total clasts), F/Qm (feldspar/monocrystalline quartz), and P/F (plagioclase/total feldspars) ratios observed for sands from the different deposition sites throughout the Holocene sedimentary record

This reduction leads to shifts in the K-Qm line in the QmKP diagram, while Qm increases. This has been observed by several authors in fluvial plutoniclastic sands (e.g. Le Pera *et al.*, 2001; Le Pera and Arribas, 2005) highlighting that the origin of fluvial sands is mainly controlled by supplies from soils developed in their drainage areas (Suttner *et al.*, 1981). These assertions concur with the high proportions of quartz grains and lesser amounts of plagioclase that fluvial sands exhibit. Taboada and García (1999) have documented the decay of plagioclase in granites by weathering in the humid climate of Galicia. In addition, coastal sands (aeolian and intertidal) show similar P/F to the mean Galician granite composition (Figure 4a), suggesting that mechanical abrasion could be the main factor responsible for the simultaneous loss of both feldspars.

These data suggest that the main origin of Galician Holocene sands is not fluvial supplies from their drainage basins, but rather supplies from cliff erosion in coastal and head deposits near the final depositional site. Sand supplies from cliff erosion may explain the fresh mineral appearance and maturity in composition due to abrasion in the absence of chemical weathering decay of feldspars in coastal sands. In addition, fluvial supplies would be extremely diluted by marine-generated sands, occluding estuarine mouths and coastal wetlands.

Conclusions

(1) The textures of Holocene sands from seven localities on the Galician and western Asturian coast mainly reflect depositional environment. Fluvial sands are texturally immature (poorly sorted and with low quartz grain roundness), while intertidal and aeolian sands exhibit mature textures (well to very well sorted and with high quartz-grain roundness). In addition, differences in composition emerge between fluvial environments and intertidal plus aeolian deposits. Modern carbonates (bioclasts) characterize marine deposits, and embayed quartz, alterites and modern silty clayey clasts are more conspicuous in fluvial sands.

(2) The ancient non-carbonate grain composition of the Galician Holocene sands indicates quartzofeldspathic petrofacies as a product of the erosion of granitoids and gneisses from the GTMZ

and CIZ of the Iberian Massif. However, differences in composition between individual localities exist, reflecting variations in local source rocks. On the Asturian coast (Navia), a quartzolithic petrofacies developed through the erosion of metasediments from the Western Asturian Leonese Zone of the Iberian Massif.

(3) Coarse-grained source rocks generate great quantities of monomineral grains (quartz and feldspars) that strongly dilute sandy supplies from other parent rocks of lower SGI. This conclusion is supported if we compare sand composition and area distributions of the lithologies at their sources.

(4) Petrographic indices such as MC/T, F/Qm and P/F are useful for analysing changes in sand composition produced during Holocene deposition. MC/T values increase because of the increased marine influence during Holocene transgression. In contrast, aeolian sands show near constant F/Qm values because of the homogenization process of reworking intertidal sands. However, fluvial and intertidal sands show a good fit of F/Qm and MC/T indices, suggesting episodes of better preservation of feldspars with greater marine supplies. In addition, plagioclase is the better-preserved feldspar in marine sands. These episodes can be associated with stages of faster sea-level rises and subsequent erosion of surrounding cliffs. In contrast, fluvial sands mainly show greater quartz enrichment.

(5) The near constant P/F in marine Holocene sands with variable quartz contents suggests that mechanical abrasion is the main factor controlling the maturity of these sands. As a consequence, the provenance of beach, intertidal and aeolian sands must be related to the erosion of coastal cliff and head deposits, with the scarce contribution of fluvial drainage supplies.

(6) Sand composition reflects local composition of its sources. Accordingly, we can rule out the long-distance transport of Galician coastal sands and infer that the rugged Galician coast produces local erosion, short transport of sediments from the west, and deposition on sediment-trap zones.

(7) Collectively our data support the idea that the origin of Holocene sands from the northwest coast of the Iberian Peninsula cannot be fluvial supplies from further inland, but rather that these sands were generated by coastal erosion of cliff and head deposits close to the final depositional site. As the Holocene transgression ensued, these deposits closed coastal wetlands and occluded estuarine mouths.

Acknowledgements

We thank A. Dawson, S. Critelli and R. Ingersoll for their comments and revision of the manuscript. This research was funded by project CGL2004-00488TE awarded by the Spanish Ministry of Science and Technology and is also a contribution to IGCP Project No. 495. Quaternary Land–Ocean interactions: Driving Mechanisms and Coastal Responses.

References

Alonso, A. and Pagés, J.L. 2000: El registro sedimentario del final del Cuaternario en el litoral noroeste de la Península Ibérica. Márgenes Cantábrico y Atlántico. *Revista de la Sociedad Geológica de España* 13, 17–29.

Alonso, A., Pagés, J.L., López García, M.J. and Cearreta, A. 2003: Cronoestratigrafía de la transgresión holocena en el Golfo Ártabro (La Coruña, NO de España). In Flor, G., editor, *Actas de la XI Reunión Nacional del Cuaternario*. Universidad de Cantabria, 33–38.

Anderson, N.J. 1995: Using the past to predict the future: lake sediments and the modelling of limnological disturbance. *Ecological Modelling* 78, 149–72.

Arenas, R., Gil Ibarguchi, J.L., González Lodeiro, F., Klein, E., Martínez Catalán, J.R., Ortega Girones, E., Pablo Maciá, J.G. and Peinado, M. 1986: Tectonostratigraphic units in the complexes with mafic and related Rocks of the NW of the Iberian Massif. *Hercynica* II, 87–110.

Arribas, J. and Tortosa, A. 2003: Detrital modes in sedimentoclastic sands from low-order streams in the Iberian Range, Spain: the potential for sand generation by different sedimentary rocks. *Sedimentary Geology* 159, 275–303.

Bao, R., Alonso, A., Delgado, C. and Pagés, J.L. 2007: Identification of the main driving mechanisms in the evolution of a small coastal wetland (Traba, Galicia, NW Spain) since its origin 5,700 cal yrBP. *Paleogeography, Paleoclimatology, Paleoecology* 247, 296–312.

Bastida, F., Marcos, A., Marquínez, J., Pérez-Estaún, A. and Pulgar, J.A. 1984: *Mapa Geológico de España E. 1:200.000. Hoja 1 La Coruña*. Instituto Geológico y Minero de España, 155 pp.

Basu, A., Young, S.W., Suttner, L.J., James, C.W. and Mack, G.H. 1975: Re-evaluation of the use of undulatory extinction and polycrystallinity in detrital quartz provenance interpretation. *Journal of Sedimentary Petrology* 45, 873–82.

Birks, H.H. 2003: The importance of plant macrofossils in the reconstruction of Lateglacial vegetation and climate: examples from Scotland, western Norway, and Minnesota, USA. *Quaternary Science Reviews* 22, 453–73.

Blatt, H., Middleton, G.V. and Murray, R.C. 1980: *Origin of sedimentary rocks*. Prentice-Hall, 634 pp.

Cameron, K.L. and Blatt, H. 1971: Durabilities of sand size schist and 'volcanic' rock fragments during fluvial transport, Elk Creek, Black Hills, South Dakota. *Journal of Sedimentary Petrology* 41, 565–76.

Cann, J.H., Murray-Wallance, C.V., Belpeiro, A.P. and Brenchley, A.J. 1999: Evolution of Holocene coastal environments near Robe, southeastern South Australia. *Quaternary International* 56, 81–97.

Castillo Rodríguez, F., Martínez Cortizas, A. and Blanco Chao, R. 2006: O clima de Galicia. In Naranjo, L. and Pérez Muñuzuri, V., coordinators, *A variabilidade natural do clima en Galicia*. Consellería de Medio Ambiente e Desenvolvemento Sostible, Xunta de Galicia, Fundación CaixaGalicia, 17–92.

Chayes, F. 1952: Notes on the staining of potash feldspar with sodium cobaltonitrite in thin section. *American Mineralogist* 37, 337–40.

Cleary, W.J. and Connolly, J.R. 1971: Distribution and genesis of quartz in a piedmont-coastal plain environment. *Geological Society of America Bulletin* 82, 2755–66.

Clemmensen, L.B., Pye, K., Murray, A. and Heinemeier, J. 2001: Sedimentology, stratigraphy and landscape evolution of a Holocene coastal dune system, Lodbjerg, NW Jutland, Denmark. *Sedimentology* 48, 3–27.

Cuesta, A. 1991: *Petrología granítica del plutón de Caldas de Reyes (Pontevedra, España): estructura, mineralogía, geoquímica y petrogénesis*. Serie Nova Terra, 5, Edicios do Castro, 363 pp.

Culver, S.J., Pre, C.A.G., Mallinson, D.J., Riggs, S.R., Corbett, D.R., Foley, J., Hale, M., Metger, L., Ricardo, J., Rosenberger, J., Smith, Ch.G., Smith, C.W., Snyder, S.W., Twamley, D., Farrell, K. and

Horton, B. 2007: Late Holocene barrier island collapse: Outer Banks, North Carolina, USA. *Sedimentary Record* 5, 4–8.

Delgado, C., Bao, R., Alonso, A. and Pagés, J.L. 2003: *Evolución paleoambiental inferida por diatomeas de la laguna costera de Traba (A Coruña, NO España) durante los últimos 5.000 años.* XI Reunión Nacional de Cuaternario, 347–352.

Dickinson, W.R., Beard, L.S., Brakenridge, G.R., Erjavec, J.L., Ferguson, R.C., Inman, K.F., Knepp, R.A., Lindberg, F.A. and Ryberg, R.T. 1983: Provenance of North American Phanerozoic sandstones in relation to tectonic setting. *Geological Society of America, Bulletin* 94, 222–35.

Di Giulio, A. and Valloni, R. 1992: Sabbie e areniti: Analisi ottica e classificazione. *Acta Naturalia Ateneo Parmense* 28, 101 pp.

Fillali, L., Arribas, J. and Garzón, G. 2005: Petrografía y morfología de los cauces fluviales y del litoral atlántico de la Península de Tánger. Análisis de procedencia en relación con la Cordillera del Rif (Marruecos). *Revista de la Sociedad Geológica de España* 18, 195–205.

Froyd, C.A. 2005: Fossil stomata reveal early pine presence in Scotland: implications for postglacial colonization analyses. *Ecology* 86, 579–86.

GarcíaAntón, M., Gil Romera, G., Pagés, J.L. and Alonso, A. 2006: The Holocene pollen record in the Villaviciosa Estuary (Asturias, North Spain). *Paleogeography, Paleoclimatology, Paleoecology* 237, 280–92.

González Lodeiro, F., Hernández Urroz, J., Martinez Catalán, J.R., Naval Balbín, A., Ortega Girones, E. and de Pablo Macia, J.G. 1984: *Mapa Geológico de España E. 1:200.000. Hoja 7 Santiago de Compostela.* Instituto Geológico y Minero de España, 99 pp.

Grantham, J.H. and Velbel, M.A. 1988: The influence of climate and topography on rock-fragment abundance in modern fluvial sands of the southern Blue Ridge Mountains, North Carolina. *Journal of Sedimentary Petrology* 58, 219–27.

Heins, W.A. 1993: Source rock texture versus climate and topography controls on the composition of modern, plutoniclastic sand. In Johnsson, M.J. and Basu, A., editors, *Processes controlling the composition of clastic sediments.* Geological Society of America, Special Paper 284, 135–46.

Hong, W., Keppens, E., Nielsen, P. and van Riet, A. 1995: Oxygen and carbon isotope study of the Holocene oyster reefs and paleoenvironmental reconstruction on the northwest coast of Bohai Bay, China. *Marine Geology* 124, 289–302.

Ibbeken, H. and Schleyer, R. 1991: *Source and sediment. A case study of provenance and mass balance at an active plate margin (Calabria, Southern Italy).* Springer, 286 pp.

Ingersoll, R.V., Bullard, T.F., Ford, R.L., Grimm, J.P., Pickle, J.D. and Sares, S.W. 1984: The effect of grain size on detrital modes: a test of the Gazzi–Dickinson point-counting method. *Journal of Sedimentary Petrology* 54, 103–16.

Johnsson, M.J. 1990: Overlooked sedimentary particles from tropical weathering environments. *Geology* 18, 107–10.

—— 1993: The system controlling the composition of clastic sediments. In Johnsson, M.J. and Basu, A., editors, *Processes controlling the composition of clastic sediments.* Geological Society of America, Special Paper 284, 1–19.

Johnsson, M.J., Stallard, R.F. and Lundberg, N. 1991: Controls on the composition of fluvial sands from a tropical weathering environment: sands of the Orinoco River drainage basin, Venezuela and Colombia. *Journal of Geology* 96, 263–77.

Krynine, P.D. 1950: Petrology, stratigraphy, and origin of the Triassic sedimentary rocks of Connecticut. *Connecticut State Geological and Natural History Survey Bulletin* 73, 247 pp.

Le Pera, E. and Arribas, J. 2005: Sand composition in an Iberian passive-margin fluvial course: the Tajo River. *Sedimentary Geology* 171, 261–81.

Le Pera, E., Arribas, J., Critelli, S. and Tortosa, A. 2001: The effects of source rocks and chemical weathering on the petrogenesis of siliciclastic sand (Calabria, Italy): implications for provenance studies. *Sedimentology* 48, 357–78.

Lindholm, R.C. and Finkelman, R.B. 1972: Calcite staining: semiquantitative determination of ferrous iron. *Journal of Sedimentary Petrology* 42, 239–45.

Lorenzo, F., Alonso, A. and Pagés, J.L. 2007: Erosion and accretion of beach and spit systems in northwest Spain: a response to human activity. *Journal of Coastal Research* 23, 834–45.

Mack, G.H. 1978: The survivability of labile light mineral grains Permian Cutler and Cedar Mesa Formations, Moab, Utah. *Sedimentology* 25, 587–606.

Marsaglia, K.M., García y Barragán, J.C., Padilla, I. and Milliken, K.L. 1996: Evolution of the Iberian passive margin as reflected in sand provenance. In Whitmarsh, R.B., Sawyer, D.S., Klaus, A. and Masson, D.G., editors, *Proceedings ODP, scientific results, 149.* Ocean Drilling Program, 269–80.

Marsaglia, K.M., Pavia, J.A. and Maloney, S.J. 2007: Petrology and provenance of Eocene–Albian sandstones and grainstones recovered during ODP Leg 210: implications for passive margin (rift-to-drift) sandstone provenance models. In Tucholke, B.E., Sibuet, J.-C. and Klaus, A., editors, *Proceedings ODP, scientific results, 210.* Ocean Drilling Program, 1–47.

Nesbitt, H.W., Fedo, C.M. and Young, G.M. 1997: Quartz and feldspar stability, steady and non-steady-state weathering, and petrogenesis of siliciclastic sands and muds. *Journal of Geology* 105, 173–91.

Pagés, J.L., Alonso, A., Cearreta, A., Hacar, M. and Bao, R. 2003: The Holocene record in the Villaviciosa Estuary (Asturias, Spain). In Ruiz Zapata, M.B., Dorado Valiño, M., Valdeolmillos Rodríguez, A., Gil García, M.J., Bardají Azcárate, T., de Bustamante Gutiérrez, I. and Martínez Mendizábal, I., editors, *Quaternary climatic changes and environmental crises in the Mediterranean region.* Universidad de Alcalá de Henares, 249–56.

Pagés, J.L., Alonso, A. and Garzón, G. 2005: Holocene transgression in the western Bay of Biscay, Spain. In Baeteman, C., editor, *INQUA – IGCP international conference. Abstract book. Late Quaternary coastal changes, sea level, sedimentary forcing and anthropogenic impacts.* Belgian Geological Survey, 77–78.

Palomares, M. and Arribas, J. 1993: Modern stream sands from compound crystalline sources: composition and sand generation index. In Johnsson, M.J. and Basu, A., editors, *Processes controlling the composition of clastic sediments.* Geological Society of America, Special Paper 284, 313–22.

Pease, P.P. and Tchakerian, V.P. 2002: Composition and sources of sand in the Wahiba sand sea, Sultanate of Oman. *Annals of the Association of American Geographers* 92, 416–34.

Pettijohn, F.J., Potter, P.E. and Siever, R. 1972: *Sand and sandstone.* Springer-Verlag, 618 pp.

Smol, J.P. and Cumming, B.F. 2000: Tracking long-term changes in climate using algal indicators in lake sediments. *Journal of Phycology* 36, 986–1011.

Suttner, L. and Dutta, P.K. 1986: Alluvial sandstone composition and climate: I. Framework mineralogy. *Journal of Sedimentary Petrology* 56, 329–45.

Suttner, L.J., Basu, A. and Mack, G.H. 1981: Climate and the origin of quartz arenites. *Journal of Sedimentary Petrology* 51, 21–29.

Taboada, T. and García, C. 1999: Pseudomorphic transformation of plagioclases during the weathering of granitic rocks in Galicia (NW Spain). *Catena* 35, 291–302.

Todd, T.W. 1968: Paleoclimatology and the relative stability of feldspar minerals under atmospheric conditions. *Journal of Sedimentary Petrology* 38, 832–44.

Tortosa, A. 1988: Análisis de las arenas actuales derivadas de rocas graníticas del Sistema Central: aplicación a los estudios de procedencia. Tesis de Licenciatura. Facultad de CC. Geológicas. Universidad Complutense de Madrid, 125 pp.

Tortosa, A., Palomares, M. and Arribas, J. 1991: Quartz grain types in Holocene deposits from the Spanish Central System: some problems in provenance analysis. In Morton, A.C., Todd, S.P. and Haughton, P.D.W., editors, *Developments in sedimentary provenance studies*. Geological Society of London Special Publication 57, 47–54.

Wilson, L. 1969: Les relations entre les processus geomorphologiques et le climatmoderne comme methode de paleoclimatologie. *Revue de Geographie Physique et de Geologie Dynamique* 11, 303–14.

Zerbini, S. 2000: Regional and local sea level variations. In Smith, D., Raper, S.B., Zerbini, S. and Sánchez-Arcilla, A., editors, *Sea level change and coastal processes. Implications for Europe*. European Commission, 81–133.

Zuffa, G.G. 1985: Optical analyses of arenites: influence of methodology on compositional results. In Zuffa, G.G., editor, *Provenance of arenites*. Reidel, 165–89.